ENVIRONMENTAL RESEARCH
COMMUNICATIONS

PAPER • **OPEN ACCESS**

Large air quality and human health impacts due to Amazon forest and vegetation fires

To cite this article: Edward W Butt *et al* 2020 *Environ. Res. Commun.* **2** 095001

Environmental Research Communications

PAPER

Large air quality and human health impacts due to Amazon forest and vegetation fires

Edward W Butt[1], **Luke Conibear**[1], **Carly L Reddington**[1], **Eoghan Darbyshire**[2,6], **William T Morgan**[2], **Hugh Coe**[2], **Paulo Artaxo**[3], **Joel Brito**[4], **Christoph Knote**[5] and **Dominick V Spracklen**[1]

[1] School of Earth and Environment, University of Leeds, Leeds, United Kingdom
[2] Centre of Atmospheric Sciences, Department of Earth and Environmental Science, University of Manchester, Manchester, United Kingdom
[3] Physics Institute, University of São Paulo, São Paulo, Brazil
[4] IMT Lille Douai, Université de Lille, SAGE, Lille, France
[5] Meteorological Institute, LMU Munich, Munich, Germany
[6] Now at: The Conflict and Environment Observatory, Hebden Bridge, HX7 5HZ, UK.

E-mail: e.butt@leeds.ac.uk

Keywords: air quality, amazon fires, PM2.5, public health

Supplementary material for this article is available online

OPEN ACCESS

RECEIVED
5 June 2020

REVISED
17 August 2020

ACCEPTED FOR PUBLICATION
19 August 2020

PUBLISHED
7 September 2020

Abstract

Vegetation fires across the tropics emit fine particulate matter ($PM_{2.5}$) to the atmosphere, degrading regional air quality and impacting human health. Extensive vegetation fires occur regularly across the Amazon basin, but there have been no detailed assessments of the impacts on air quality or human health. We used updated exposure-response relationships and a regional climate-chemistry model, evaluated against a comprehensive set of observational data, to provide the first in-depth assessment of the potential public health benefits due to fire prevention across the Amazon Basin. We focused on 2012, a year with emissions similar to the 11-year average (2008 to 2018). Vegetation fires contributed >80% of simulated dry season mean surface $PM_{2.5}$ in the western Amazon region particularly in Bolivia and Brazilian states of Rondônia, Acre, and Mato Grosso. We estimate that the prevention of vegetation fires would have averted 16 800 (95UI: 16 300–17 400) premature deaths and 641 000 (95UI: 551 900–741 300) disability adjusted life years (DALYs) across South America, with 26% of the avoided health burden located within the Amazon Basin. The health benefits of fire prevention in the Amazon are comparable to those found in Equatorial Asia.

1. Introduction

Vegetation and peat fires are an important source of particular matter (PM) and trace gases to the atmosphere, which can degrade regional air quality and adversely impact human health. Ambient $PM_{2.5}$ (PM with an aerodynamic median diameter less than 2.5 μm) is a leading risk factor contributing to mortality, morbidity and reduced life expectancy (Cohen *et al* 2017, Apte *et al* 2018). Exposure to $PM_{2.5}$ from vegetation and peat fires is estimated to cause 179 000–339 000 premature deaths each year, equivalent to 5% of the present-day global burden of disease due to ambient $PM_{2.5}$ exposure (Johnston *et al* 2012, Lelieveld *et al* 2015). Fires in tropical and sub-tropical regions are responsible for 90% of global $PM_{2.5}$ fire emissions (Wiedinmyer *et al* 2011, Van Der Werf *et al* 2017), and fires are the dominant source of PM pollution across much of the tropics (Johnston *et al* 2012, Lelieveld *et al* 2015).

Fires in the tropics are influenced by both climate and land-use change (Heald and Spracklen 2015). Drought increases the incidence of fire in the Amazon (Arãgao *et al* 2008, da Silva *et al* 2018, Aragão *et al* 2018). Fire is used across the tropics to clear forest and other vegetation and prepare land for agriculture. In the Amazon, fire emissions are greater in years with higher deforestation rates (Arãgao *et al* 2008, Reddington *et al* 2015). Deforestation and forest degradation (Morgan *et al* 2019b) result in a fragmented forest landscape that is

increasingly prone to fire (Cano-Crespo *et al* 2015, Alencar *et al* 2015). Deforestation also alters regional climate, increasing local temperatures (Baker and Spracklen 2019) and reducing regional rainfall (Spracklen *et al* 2012, Spracklen and Garcia-Carreras 2015, Zemp *et al* 2017). Smoke from fires further reduces rainfall through interactions with clouds and radiation (Kolusu *et al* 2015, Archer-Nicholls *et al* 2016, Liu *et al* 2020). Positive feedbacks between deforestation, drought, fire and smoke exacerbate the potential for tipping points in the Amazon climate (Nepstad *et al* 2008, Lovejoy and Nobre 2018).

Vegetation fires are the dominant source of PM over the Amazon (Martin *et al* 2010, Mishra *et al* 2015). The Amazon exhibits a strong seasonal cycle in vegetation fires and consequently PM concentrations (Martin *et al* 2010). During the wet season when there is little fire activity, $PM_{2.5}$ concentrations across central Amazonia can be as low as 1.5 $\mu g\,m^{-3}$ (Artaxo *et al* 2013). In contrast, during the dry season (August–October) when there are a large number of vegetation fires, regional dry season mean $PM_{2.5}$ concentrations can exceed 30 $\mu g\,m^{-3}$ (Artaxo *et al* 2013, Reddington *et al* 2016, Reddington *et al* 2019b) with daily mean peak concentrations exceeding 100 $\mu g\,m^{-3}$ (Brito *et al* 2014). Global modelling studies confirm that fires are a dominant source of regional $PM_{2.5}$ concentrations across the Amazon during the dry season (Johnston *et al* 2012, Lelieveld *et al* 2015, Reddington *et al* 2015, Reddington *et al* 2016, Reddington *et al* 2019b).

There is strong evidence of acute adverse health outcomes due to exposure to PM from Amazon fires. Positive associations between PM from vegetation fires and increased hospital admissions for respiratory health in children and the elderly have been demonstrated in the southern Amazon (Ignotti *et al* 2010, Do Carmo *et al* 2013, Machado-Silva *et al* 2020). PM from fires has also been found to exacerbate respiratory health in children and the elderly to a greater extent during drought years (Smith *et al* 2014, Machado-Silva *et al* 2020). The relationship between respiratory health and PM from fires has also been highlighted by positive associations between reduced peak expiratory flow in schoolchildren and increased PM during the dry season (Jacobson *et al* 2012, Jacobson *et al* 2014). Toxicology analysis has demonstrated PM from Amazon fires results in DNA damage in human lung cells (de Oliveira Alves *et al* 2017), shedding light on the mechanisms by which exposure to PM from vegetation fires adversely impact human health.

Despite studies demonstrating the impact of PM from fires on human health there have been no regional assessments quantifying the potential health burden using high resolution models. Previous studies of PM from vegetation fires have focused on the impacts on Amazonian weather and climate through aerosol-radiation and aerosol-cloud interactions (Zhang *et al* 2008, Zhang *et al* 2009, Wu *et al* 2011, Kolusu *et al* 2015, Archer-Nicholls *et al* 2016, Thornhill *et al* 2018, Liu *et al* 2020). Health burden assessment of the degraded air quality caused by Amazon fires have been restricted to coarse resolution global models (>100 km horizontal resolution) (Johnston *et al* 2012, Lelieveld *et al* 2015, Reddington *et al* 2015, Nawaz and Henze 2020) with limited in-depth analysis at a regional scales at finer resolutions. In comparison, Equatorial Asia, where vegetation and peat fires also result in poor regional air quality, has been studied in detail (Huang *et al* 2013, Reddington *et al* 2014, Kim *et al* 2015, Marlier *et al* 2015, Kiely *et al* 2019) and there are numerous assessments of the health burden. Reddington *et al* (2019a) found that the elimination of vegetation fires would avert 8 000 premature deaths annually across Southeast Asia (Myanmar, Thailand, Laos, Cambodia, and Vietnam). Marlier *et al* (2019) found the elimination of fires across Equatorial Asia (Indonesia, Malaysia, and Singapore) had the potential to avert 24 000 premature deaths per year. Similarly, Kiely *et al* (2020) estimated that the prevention of fires across Indonesia would avert an average of 15 000 premature deaths annually in 2004, 2006, and 2009. A number of studies focused on 2015, when drought conditions caused extensive fires and a major haze event, resulting in an estimated 44 000–100 300 premature mortalities across Equatorial Asia (Crippa *et al* 2016, Koplitz *et al* 2016, Kiely *et al* 2020). Here we quantify the impact of vegetation fires in South America on regional air quality and human burden of disease, with a focus on the Amazon. We used a high spatial resolution regional climate-chemistry model, evaluated against a comprehensive set of observational data to improve understanding of the magnitude and spatial distribution of simulated air pollutants from vegetation fires. We then used exposure-response relationships to provide an in-depth assessment of the burden of disease associated with exposure to $PM_{2.5}$ from vegetation fires. Our findings provide advancement on previous air quality and health assessments within this region by combining a state-of-the-art high resolution climate-chemistry model with newly established exposure-response relationships.

2. Methods

2.1. Model description

We used the Weather Research and Forecasting online-coupled Chemistry model (WRF–Chem) version 3.7.1 (Grell *et al* 2005). The model domain covers most of South America (figure 1) with a horizontal resolution of 30 km, extending vertically from the surface to 10 hPa. Details of model setup are shown in supplementary table 1 is available online at stacks.iop.org/ERC/2/095001/mmedia.

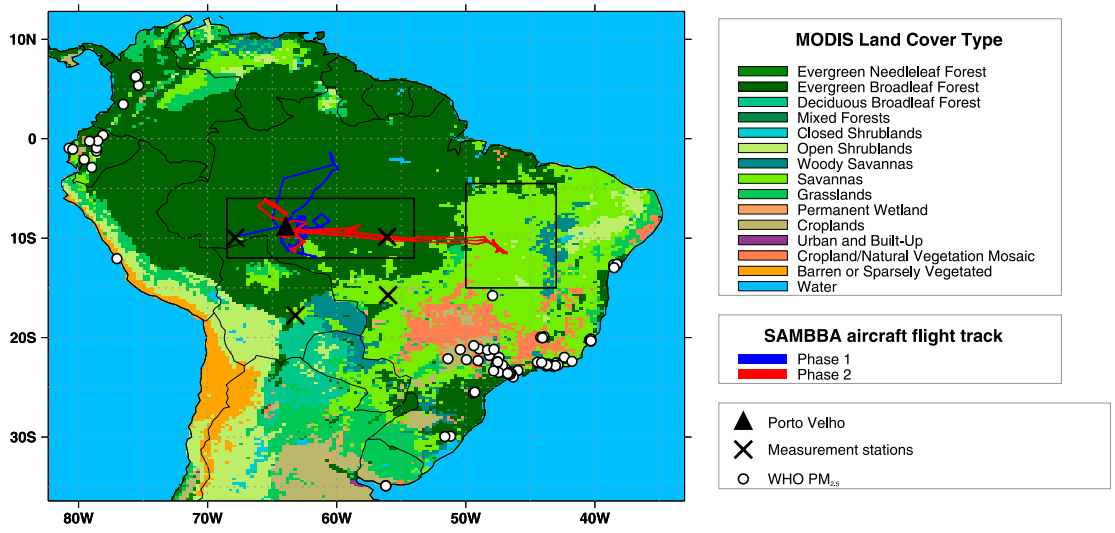

Figure 1. The WRF-Chem model domain used in the study and associated land cover classification depicted by the MODIS Land Cover Type Data Product (MCD12Q1) International Geosphere-Biosphere Programme (IGBP). Flight tracks during the SAMBBA campaign are shown (Phase 1: 13–23 September; blue line, and Phase 2: 23 September–3 October 2012; red line). The eastern (4.5–15 °S, 43–50 °W) and western (6–12 °S, 54–68.5 °W) domains used for flight track evaluation are shown with black boxes. The location of the Porto Velho ground station is represented by a solid black triangle. Locations of AERONET stations are shown by the black crosses: Porto Velho UNIR (8.84 °S, 63.94 °W), Alta Floresta (9.87 °S, 56.10 °W), Rio Branco (9.96 °S, 67.87 °W), Cuiabá-Miranda (15.73 °S, 56.02 °W) and Santa Cruz UTEPSA (17.77 °S, 63.20 °W). White circles show the locations of annual $PM_{2.5}$ measurements from the WHO database.

Gas-phase chemistry is calculated using the extended Model for Ozone and Related Chemical Tracers, version 4 (MOZART-4) (Emmons *et al* 2010, Knote *et al* 2014). Aerosol chemistry and microphysics is simulated using an updated Model for Simulating Aerosol Interaction and Chemistry (MOSAIC) with aqueous chemistry and four sectional discrete aerosol size bins: 0.039–0.156 μm, 0.156–0.625 μm, 0.625–2.5 μm, 2.5–10 μm (Zaveri *et al* 2008, Hodzic and Knote 2014). An updated volatility basis set mechanism was also included for secondary organic aerosol (SOA) formation (Knote *et al* 2015).

Microphysics is simulated using the Morrison 2-moment scheme (Morrison *et al* 2009) and the Grell 3D parameterisation is used for simulating convection (Grell and Dévényi 2002). Initial and boundary chemistry and aerosol conditions were taken from 6-hourly simulation data from the MOZART-4/Goddard Earth Observing System Model version 5 (GEOS5) (NCAR 2019). Initial and boundary meteorological conditions were taken from the European Centre for Medium–Range Weather Forecasts (ECMWF) global reanalysis (Dee *et al* 2011)

During model simulations, we nudged the meteorological components, horizontal and vertical wind, potential temperature and water vapour mixing ratio, to ECMWF re-analysis in all model levels above the planetary boundary layer over 6 h.

2.2. Model simulations

WRF-Chem simulations were conducted for the year 2012 at horizontal resolution of 30 km. We focused on the dry season (defined here as August 1st to October 31st) when vegetation fires are most active. We performed simulations from April to December, discarding the first month as model spin-up. We performed two types of simulations: one simulation excluding fire emissions ('fire_off') and one simulation including vegetation fire emissions ('fire_on'). The contribution of fires to $PM_{2.5}$ was calculated as the difference in concentrations between these two simulations.

2.2.1. Non-fire emissions

Anthropogenic emissions were taken from the Emission Database for Global Atmospheric Research with Task Force on Hemispheric Transport of Air Pollution (EDGAR-HTAP) version 2.2 for the year 2010 at $0.1^\circ \times 0.1^\circ$ horizontal resolution (Janssens-Maenhout *et al* 2015). A diurnal cycle was applied to anthropogenic emissions based on Olivier *et al* (2003). Biogenic volatile organic compound (VOC) and dust emissions were both calculated online by the Model of Emissions of Gases and Aerosol from Nature (MEGAN) (Guenther *et al* 2006) and through Goddard Global Ozone Chemistry Aerosol Radiation and Transport (GOCART) with Air Force Weather Agency (AFWA) modification (Chin *et al* 2000), respectively.

Table 1. Domain wide and Amazon Basin annual and dry season (August–October) total organic carbon (OC) and black carbon (BC) emissions from FINN (v1.5). Emissions in 2012 are compared against the 11-y (2008 to 2018) average in parentheses.

Emission species	Annual domain (Tg a^{-1})	Dry season domain (Tg a^{-1})	Amazon Basin annual	Amazon Basin dry season
OC	3.6 (3.1)	2.6 (2.0)	2.4 (2.1)	1.8 (1.5)
BC	0.4 (0.3)	0.3 (0.2)	0.3 (0.2)	0.2 (0.2)

2.2.2. Fire emissions

We used fire emissions from the Fire Inventory from NCAR (FINN) version 1.5 (Wiedinmyer *et al* 2011) (see list of emissions species in supplementary table 2). Daily emissions are estimated on a 1 km^2 grid based on the location and timing of active fires taken from the Moderate Resolution Imaging Spectroradiometer (MODIS) Fire and Thermal Anomalies Product (Giglio *et al* 2003). Each fire count is assigned a burned area (0.75 km^2 for grassland and savannah and 1 km^2 for other land covers). To account for missing fire retrievals due to cloud cover, FINN averages fire emissions over two days, assuming that the detected burned area will be half the original size the following day (Wiedinmyer *et al* 2011, Pereira *et al* 2016). Trace gas and aerosol emissions are calculated using emission factors (Akagi *et al* 2011, 2013, Yokelson *et al* 2013) in conjunction with MODIS Land Cover Type and Vegetation Continuous Fields. Fire emissions are emitted with a diurnal cycle that peaks in the early afternoon (local-time) based on Giglio (2007).

Buoyancy due to fire plumes can cause rapid injection of fire emissions above the ground surface (e.g., Fromm *et al* 2000). WRF-Chem can simulate this plume-rise from fires (e.g., Freitas *et al* 2007). However, previous modelling studies of Amazon fires during the dry season of 2012 shows this method overestimates the height of fire plumes (Archer-Nicholls *et al* 2015, Archer-Nicholls *et al* 2016). Observational work also found very little evidence of extensive elevated layers during the same simulation period, suggesting little evidence of pyroconvection (Darbyshire *et al* 2019). We therefore inject vegetation fire emissions evenly throughout the boundary layer (BL) (e.g., Dentener *et al* 2006), as supported by analysis of plume heights over the Amazon (Marenco *et al* 2016, Gonzalez-Alonso *et al* 2019).

Table 1 shows annual and dry season organic carbon (OC) and black carbon (BC) emissions from FINN v1.5 summed over our modelling domain. Emissions are dominated by OC, which contributes 90% of OC + BC emissions. In 2012, domain wide annual OC + BC emissions were 4 Tg a^{-1}, approximately 17% greater than the 11-y (2008 to 2018) average (3.4 Tg a^{-1}). The domain contributes 17% of global fire BC + OC emissions during 2008 to 2018 (figure 2(d)), highlighting the importance of fires in this region. Emissions are dominated by dry season fires, which account for 65% of annual OC emissions over the 11-y average. Fire emissions are greatest in southern areas of the Amazon (figures 2(a), (b)) which are undergoing land-use change. During 2008 to 2018, the Amazon accounted for 66% (72%) of annual (dry season) domain total OC emissions (table 1). Compared to the 11-y average, fire emissions in 2012 were enhanced across the Brazilian and Peruvian Amazon, but were lower across the Bolivian Amazon (figure 2(c)). Emissions were also higher in the eastern Cerrado region of Brazil in 2012 compared to the 11-y average, as supported by observed enhancement in Cerrado active fires in this region (supplementary figure 1). Previous work comparing FINN (v1.5) to the Global Fire Assimilation System (GFAS) (Kaiser *et al* 2012) and Global Fire Emissions Dataset (GFED) (v4s) (Van Der Werf *et al* 2017) in 2012, showed that emissions datasets had broadly similar spatial patterns of BC and OC emissions over the Amazon region. Emissions in FINN were greater compared to GFED and GFAS over western regions and lower compared to other datasets over eastern regions (Reddington *et al* 2019b). Comparison against measured aerosol concentrations suggested that GFED and GFAS emissions may be underestimated in the western Amazon and all emission datasets may underestimate in the eastern Amazon (Reddington *et al* 2019b).

2.3. Measurements

We evaluate our WRF-Chem simulations against a comprehensive set of observational datasets from surface and aircraft collected as part of the South American Biomass Burning Analysis (SAMBBA) field campaign, which took place over the southern Amazon in September and October 2012 (Johnson *et al* 2016, Reddington *et al* 2019b). We compliment SAMBBA observations with additional surface and satellite measurements.

2.3.1. Statistical methods

In order to compare WRF-Chem to measurements, we linearly interpolated model output to the time and location of measured data. Comparison to aerosol mass measurements was conducted using simulated mass within the instrument detection ranges. Model evaluation was quantified using Pearson correlation coefficient (r), mean bias (MB) and normalised mean bias factor (NMBF) (Yu *et al* 2006):

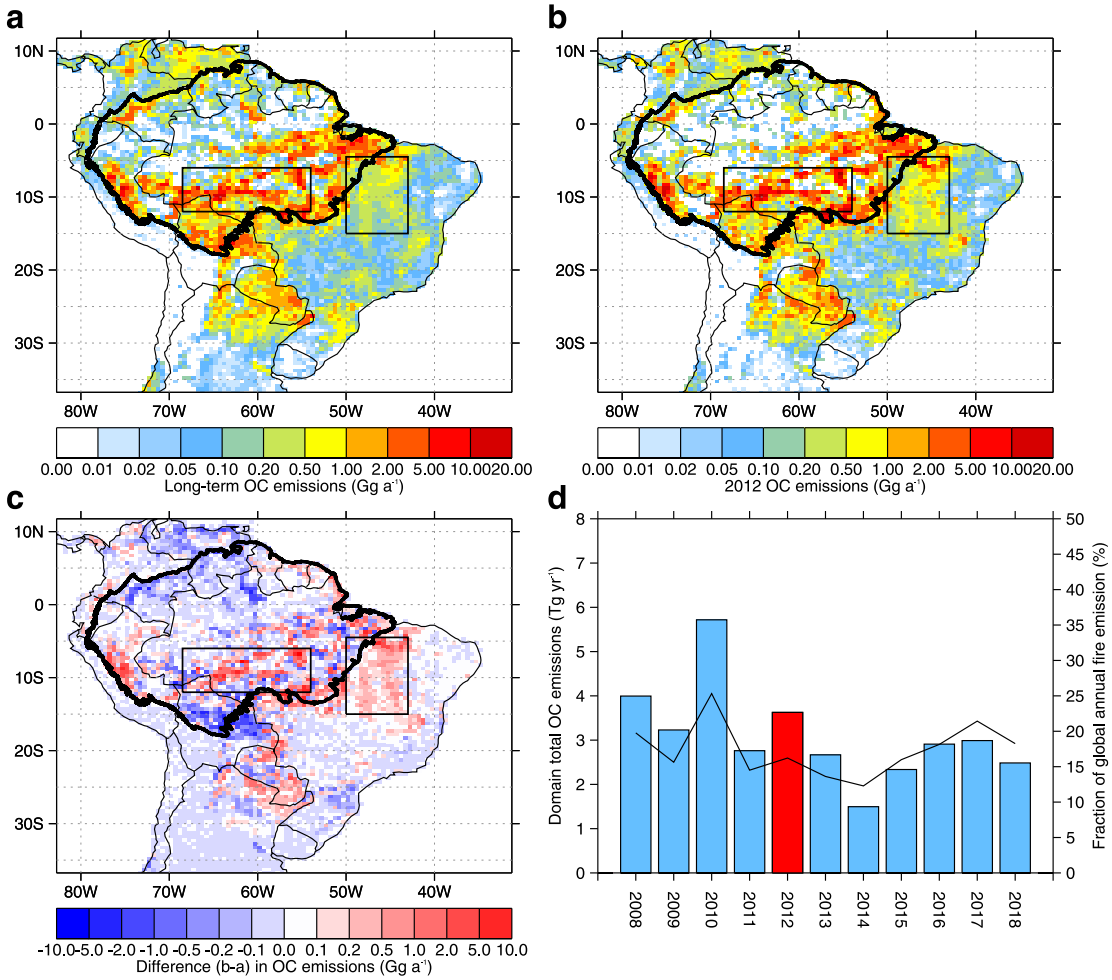

Figure 2. Annual organic carbon (OC) fire emissions from FINNv1.5 for (a) 2008 to 2018 average, (b) 2012, (c) 2012 minus 2008–2018 average. The black polygon in a-c marks the Amazon Basin. Black boxes in a-c are the western and eastern regions used in this analysis. (d) Domain wide annual OC emissions (bars) and the fraction of global fire emissions (OC + BC) contributed by the domain (black line). FINN emissions have been gridded to 0.5° × 0.5° resolution.

$$MB = \frac{1}{N}\sum_{i=1}^{N}(Mi - Oi)$$
$$NMBF = \frac{\sum(Mi - Oi)}{\sum Oi} \; if \; \overline{M} \geqslant \overline{O} \; or$$
$$NMBF = \frac{\sum(Mi - Oi)}{\sum Mi} \; if \; \overline{M} < \overline{O} \qquad (1)$$

where M and O are the model and observation value at location and timestep i. MB shows the deviation of the model to observation in the same units. NMBF is unitless and is interpreted as a factor NMBF + 1 by which the model under or overestimates the observation.

2.3.2. Surface measurements

We used surface particulate matter (PM) measurements from a forested site in south-western Amazon 5 km upwind from the city of Porto Velho (population of around 500 000) (Brito *et al* 2014) (figure 1). Composition resolved aerosol mass are available from an Aethalometer (Magee Scientific, model AE30) and an aerosol chemical speciation monitor (ACSM). The Aethalometer measured equivalent black carbon (BC) at a 5 min resolution, while the ACSM measured ammonium (NH4), nitrate (NO3), sulfate (SO4), chloride (Cl) and organic mass concentration in the 75–650 nm size range at a 30 min resolution. Measurements from both instruments were available from 6th September to 1st October 2012. Details regarding measurement uncertainty for both instruments can be found in Brito *et al* (2014) and Reddington *et al* (2019b). $PM_{2.5}$ mass concentrations from a gravimetric filter analysis were used from May to October 2012, with a temporal resolution ranging 1 to ~7 days (Artaxo *et al* 2013). Annual mean $PM_{2.5}$ measurements for 2012 were taken from

the World Health Organisation (WHO) Ambient Air Quality Database 2018 Update (WHO 2018) (figure 1). The WHO database is compiled such that $PM_{2.5}$ are representative of annual mean city and town level concentrations using measurements from urban background locations. For consistency, $PM_{2.5}$ concentrations were estimated using PM10:$PM_{2.5}$ conversion factors at locations where PM10 measurements were only available (WHO 2018). We used WHO $PM_{2.5}$ measurements from Brazil, Bolivia, Colombia, Ecuador, Peru, Paraguay and Uruguay (supplementary table 3).

2.3.3. Aircraft measurements

We used aerosol measurements taken during flights of the Facility for Airborne Atmospheric Measurements (FAAM) BAe-146 research aircraft as part of the SAMBBA campaign (Johnson *et al* 2016, Darbyshire *et al* 2019, Reddington *et al* 2019b). Measurements included organic aerosol (OA) in the 50–750 nm size range from an aerosol mass spectrometer (AMS) (Canagaratna *et al* 2007, Allan *et al* 2014) and refractive BC taken from a single-particle soot photometer (SP2) (Stephens *et al* 2003, Allan *et al* 2014). FAAM flight track paths are shown in figure 1. Following Johnson *et al* (2016) and Reddington *et al* (2019b), we split analysis of profile measurements into SAMBBA Phase 1 (13–22 September 2012; flights 1–8) and Phase 2 (23 September–3 October; flights 9–20), and by western region and eastern region (figure 1). We note, however, the smaller number of flights in the eastern region (one full flight and sections of three flights) compared to the western region (14 full flights and sections of 5 flights). To avoid additional data biases, data were removed when the FAAM aircraft were sampling in-plumes and within clouds, see Darbyshire *et al* (2019) for more details.

2.3.4. Aerosol optical depth measurements

We used spectral columnar aerosol optical depth (AOD) data from the Aerosol Robotic Network (AERONET) Cimel sun photometers (Holben *et al* 1998). We used Version 3 Level 2 cloud-screened and quality-assured daytime average AOD data (Giles *et al* 2019), retrieved at 500 nm at five stations located across the Amazon Basin (figure 1). Measurements were taken at 12:00 UTC.

Satellite-derived AOD was obtained from Moderate resolution Imaging Spectroradiometer (MODIS) on Aqua (MYD04_L2) and Terra (MOD04_L2) satellites. Collection 6.1, level 2, AOD was acquired at 550 nm for the dataset 'Dark Target Deep Blue Combined' (Levy *et al* 2013). Swaths of 10 km (at nadir) were resampled to $0.1^\circ \times 0.1^\circ$ resolution. Data were aggregated to daily means. Because daytime overpass times are different for both Terra (10:30 LT) and Aqua (13:30 LT), we used model simulated AOD averaged between both overpass times and evaluated only on days when satellite data were available.

2.3.5. Radiosonde measurements

We used radiosonde measurements of potential temperature, water mixing ratio, relative humidity, wind speed and direction taken from the University of Wyoming database of radiosonde measurements (http://weather.uwyo.edu/upperair/sounding.html). Atmospheric sounding data were obtained at 12:00 UTC at 3 stations within the Amazon Basin: Porto Velho UNIR, Alta Floresta and Cuiabá-Miranda. At all 3 locations, WRF-Chem performs reasonably at simulating key atmospheric variables potential temperature, water mixing ratio, relative humidity, wind speed and direction (NMBF $= -0.24$ to 0.14, r $= 0.7$ to 0.99) during the dry season (supplementary figure 2).

2.4. Health burden calculation

We used simulated annual mean surface $PM_{2.5}$ concentrations to quantify the health impact due to fires through the disease burden attributable to air pollution exposure. To estimate annual mean $PM_{2.5}$ we assumed simulated concentrations in May and December are representative of January–April, when fire emissions are also low.

Using population attributable fractions of relative risk taken from associational epidemiology, intervention–driven variations in exposure (i.e., population exposure including and excluding vegetation fires) were used to predict associated variations in health burden outcomes. The population attributable fraction (PAF) was estimated as a function of population (P) and the relative risk (RR) of exposure:

$$PAF = P \times (RR_{EXP} - 1/RR_{EXP}) \quad (2)$$

The RR was estimated through the Global Exposure Mortality Model (GEMM) (Burnett *et al* 2018). We used the GEMM for non–accidental mortality (non–communicable disease, NCD, plus lower respiratory infections, LRI), using parameters including the China cohort, with age–specific modifiers for adults over 25 years of age in 5–year intervals. The GEMM functions have mean, lower, and upper uncertainty intervals. The theoretical minimum-risk exposure level for the GEMM functions is 2.4 $\mu g\ m^{-3}$. The toxicity of $PM_{2.5}$ was treated as homogenous with no differences for source, shape, or chemical composition, due to a lack of associations among epidemiological studies.

The effect of air pollution is known to be significantly different for morbidity and mortality from cardiovascular outcomes (IHD and STR) (Cohen *et al* 2017), and the relative risks from equation (1) were adjusted by equation (2) ($RR_{adjusted}$) when estimating years lived with disability (YLD). The ratio for IHD and STR morbidity were 0.141 and 0.553 from the GBD2016 (Cohen *et al* 2017), based on data from three cohort studies (Miller *et al* 2007, Puett *et al* 2009, Lipsett *et al* 2011)

$$RR_{EXP,adjusted} = ratio \times RR_{EXP} - ratio + 1 \tag{3}$$

Premature mortality (MORT), years of life lost (YLL), and years lived with disability (YLD) per health outcome, age bracket, and grid cell were estimated as a function of the PAF and corresponding baseline mortality (I_{MORT}), YLL (I_{YLL}), and YLD (I_{YLD}) following equations (3)–(5), respectively.

$$MORT = PAF \times I_{MORT} \tag{4}$$

$$YLL = PAF \times I_{YLL} \tag{5}$$

$$YLD = PAF \times I_{YLD} \tag{6}$$

Disability–adjusted life years (DALYs), i.e. the total loss of healthy life, was estimated as the total of YLL and YLD:

$$DALYs = YLL + YLD \tag{7}$$

The rates of MORT, YLL, YLD, and DALYs were calculated per 100,000 population. Mean estimates were quantified in addition to upper and lower uncertainty intervals at the 95% confidence level. The United Nations adjusted population count dataset for 2015 at $0.25^\circ \times 0.25^\circ$ resolution was obtained from the Gridded Population of the World, Version 4 (GPWv4) (Doxsey-Whitfield *et al* 2015). Population age composition was taken from the GBD2017 for 2015 for early–neonatal (0–6 days), late–neonatal (7–27 days), post–neonatal (8–364 days), 1–4 years, 5 to 95 years in 5–year intervals, and 95 years plus (Global Burden of Disease Study 2017, 2018). Shapefiles were used to aggregate results at the country and state level (Hijmans *et al* 2012).

The health impacts of $PM_{2.5}$ depend non-linearly on exposure, with impacts starting to saturate at high $PM_{2.5}$ concentrations. We estimate the health benefits that would arise if fires were prevented, as the health burden from a scenario with fires (fire_on) minus the health burden from a scenario without fires (fire_off) (but including other emission sources). This is described as the 'subtraction' method (Kodros *et al* 2016, Conibear *et al* 2018).

3. Results and discussion

3.1. Surface PM

Figure 3 shows measured and simulated surface aerosol mass concentrations at Porto Velho, a location heavily influenced by vegetation fires. Before the dry season (May to July), measured $PM_{2.5}$ concentrations are typically less than 3 $\mu g\,m^{-3}$, peaking at 30–50 $\mu g\,m^{-3}$ in August and September, followed by a decline in early October to less than 10 $\mu g\,m^{-3}$ (figure 3(a)). The model captures this seasonal cycle relatively well (r = 0.57), but overestimates concentrations (NMBF = 0.72, MB = 7.6 $\mu g\,m^{-3}$) largely due to an over prediction from mid-August to September. Simulated $PM_{2.5}$ concentrations are underestimated in early August, possibly due to the missing fires at the start of the dry season in the FINN dataset (Reddington *et al* 2019b). Vegetation fires contributed ~86% to simulated $PM_{2.5}$ concentrations in August and September. In the simulation without fires, $PM_{2.5}$ concentrations remain below 3 $\mu g\,m^{-3}$ throughout May to December. At urban locations far from the fires, the model simulates annual mean surface $PM_{2.5}$ concentrations to within 25% (supplementary figure 3; NMBF = −0.26, MB = −3.47 $\mu g\,m^{-3}$).

During the SAMBBA campaign, measured concentrations of OA, BC and total aerosol mass show a decline in mass concentrations towards the end of the dry season, from 13th to 30th September 2012 (figure 3(b)). Overall, the model also overestimates OA (NMBF = 0.87), BC (NMBF = 0.2) and total aerosol mass (NMBF = 0.87) in September (figure 3(b)). The model performs better during SAMBBA Phase 1 (OA NMBF = 0.36; BC NMBF = 0.03; total aerosol mass NMBF = 0.37), compared to Phase 2 (OA NMBF = 3.51; BC NMBF = 0.60; total aerosol mass NMBF = 3.05). Measured and simulated aerosol mass (not shown) are dominated by OA (measured: 78.7%, model: 83.6%), with smaller contribution from BC (measured: 11.5%, model: 5.8%), and inorganics ($NH_4 + NO_3 + Cl + SO_4$; measured: 9.8%, model: 10.6%). Analysis of OA:CO ratios in biomass burning smoke during the SAMBBA campaign suggests limited net gain of OA mass from secondary processes within fire plumes (Brito *et al* 2014, Morgan *et al* 2019a). We also find limited additional mass due to SOA formation, with SOA contributing <15% to simulated OA mass at Porto Velho.

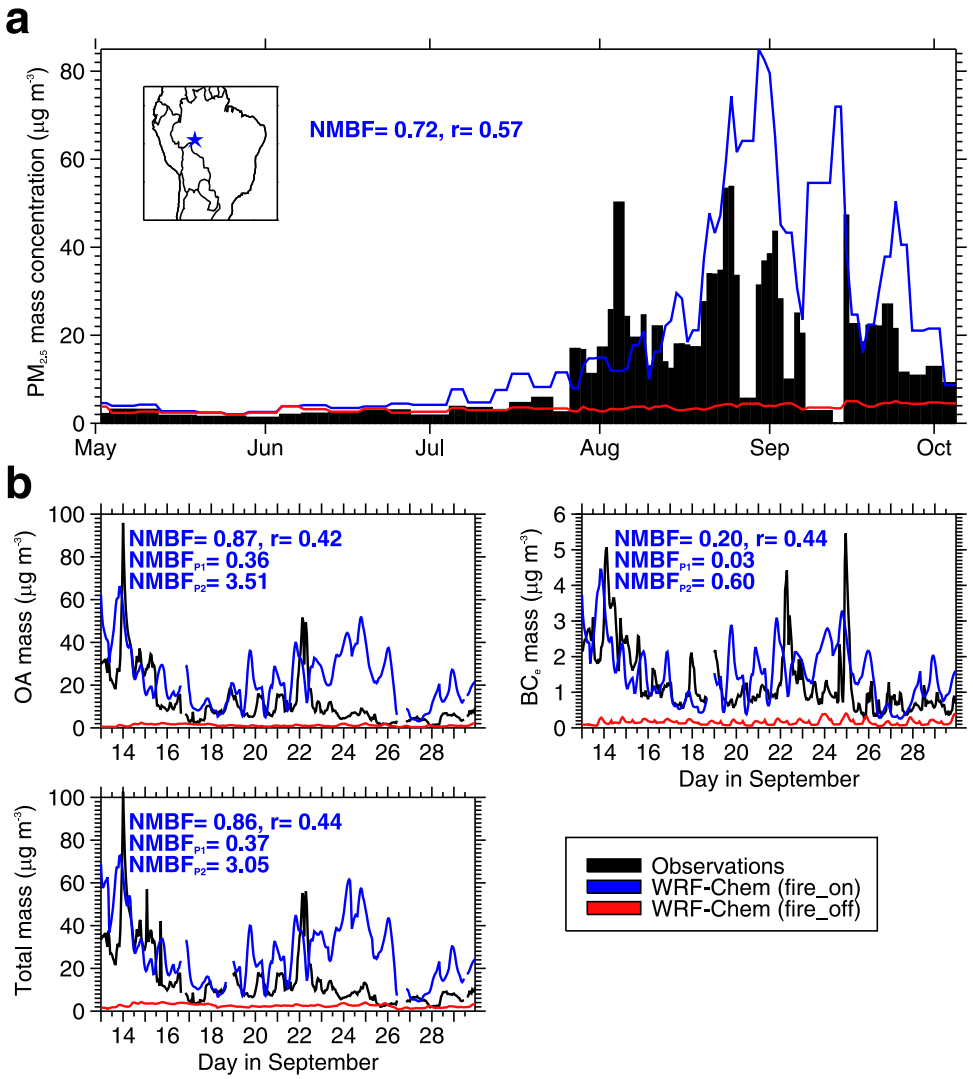

Figure 3. Comparison of simulated and measured particulate matter concentrations at Porto Velho. (a) Time-series of mean $PM_{2.5}$ between May and October 2012. Observed and simulated $PM_{2.5}$ concentrations are averages over measurement sampling periods ranging from 1 to 7 d. (b) Hourly mean concentrations during the SAMBBA campaign (13th to 30th September 2012). Measurements of OA by ACSM, BC equivalent by aethalometer, and total mass including ACSM OA, nitrate, ammonium, chloride, sulfate and aethalometer BC (OA + NO_3 + NH_4 + Chl + SO_4 + BC). Normalised mean bias factors are provided overall (NMBF) and for SAMBBA Phase 1 ($NMBF_{P1}$) and Phase 2 ($NMBF_{P2}$).

3.2. Vertical profile

Figure 4 shows simulated and measured vertical profiles of OA and BC mass taken during the SAMBBA flight campaign. Following previous studies (e.g., Archer-Nicholls *et al* 2015, Reddington *et al* 2019b), we separate analysis into SAMBBA Phase 1 and Phase 2, and into western and eastern regions (section 2.3.3). Measured aerosol mass concentrations are greater in the lower 2.5 km in the west and the lower 4 km in the east, with concentrations rapidly declining above. Simulated concentrations capture the shape of the observed vertical profile ($r \geqslant 0.9$), showing that distributing fire emissions through the BL is a reasonable assumption.

In the western Amazon, simulated BL concentrations of both BC and OA are in generally good agreement with observations (NMBF $\leqslant 0.15$). Measured OA and BC concentrations show a reduction between Phase 1(OA: 15 $\mu g\,m^{-3}$; BC: 1 $\mu g\,m^{-3}$) and Phase 2 (OA: 7 $\mu g\,m^{-3}$; BC: 0.6), consistent with the decline in measured surface concentrations at Porto Velho (figure 3). The model simulates this reduction in OA (observations: −56%; model: −58%) and BC (observations: −38%; model: −30%) concentrations, coinciding with the dry-to-wet-season transition. Previous modelling studies have struggled to simulate this observed reduction in the western Amazon, potentially due to poor simulation of wet removal of aerosols (Archer-Nicholls *et al* 2015, Reddington *et al* 2019b).

For the eastern region, simulated concentrations in the BL are underestimated (OA NMBF = −0.66; BC NMBF = −6.32), consistent with a previous study (Reddington *et al* 2019b). Measured BC:OA ratios in the BL are greater in the eastern region (0.16) compared to the western region (around 0.1). This may be caused by

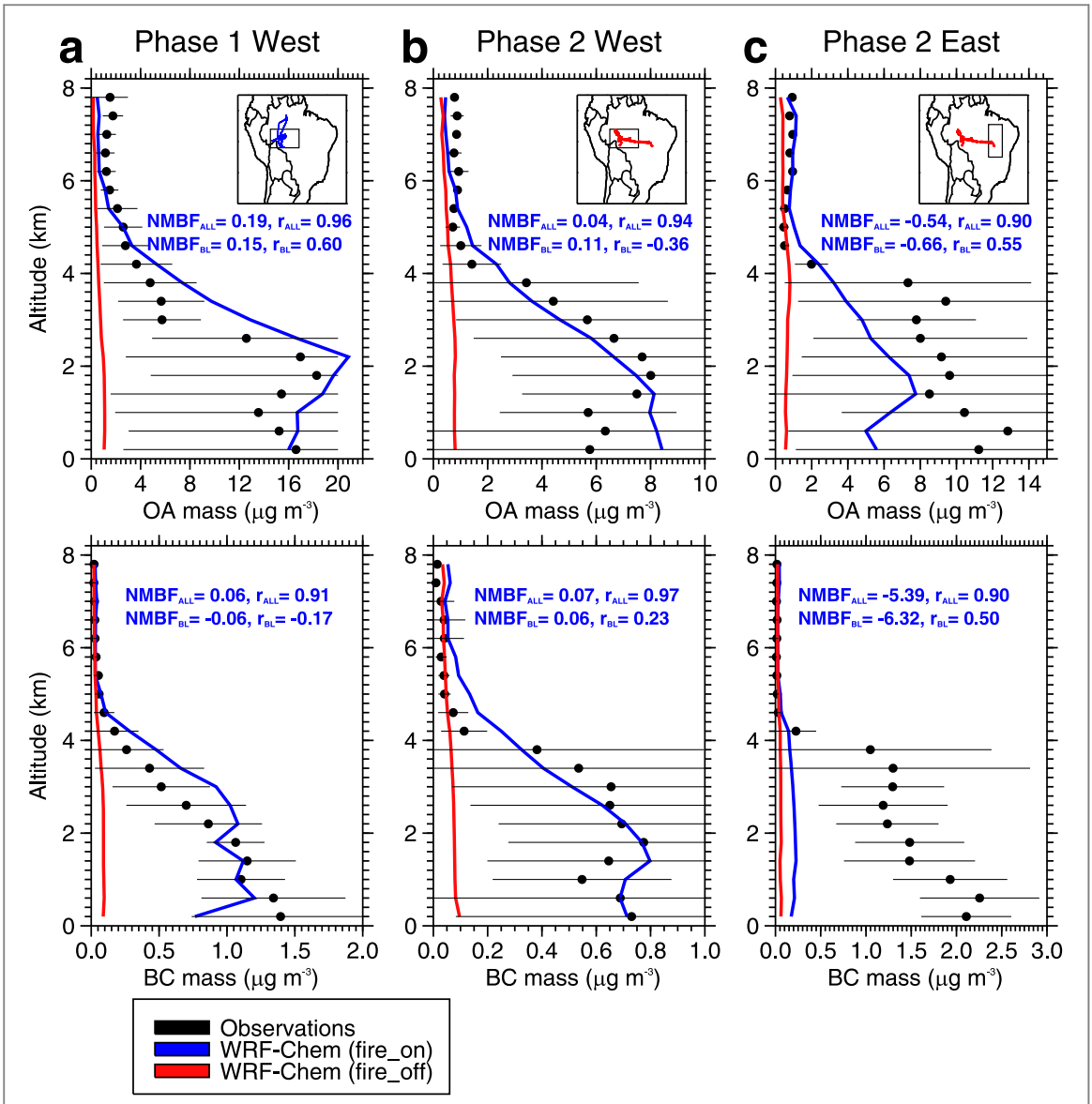

Figure 4. Mean observed (black circles) and simulated (coloured line) vertical profiles of OA and BC taken during the SAMBBA aircraft campaign. (a) Western Amazon during Phase 1 (Phase 1: 13–22 September 2012). (b) Western Amazon during Phase 2 (Phase 2: 23 September–3 October 2012). (c) Eastern Amazon (Phase 2). Inset maps show the western and eastern regions and flight paths (see also figure 1). Error bars show the standard deviation of the measurements. NMBF and correlation coefficient are shown for entire vertical profile ($NMBF_{ALL}$ and r_{ALL}), and within the PBL ($NMBF_{BL}$ and r_{BL}).

higher BC emission factors of flaming savannah fires in eastern Cerrado regions relative to the smouldering fires typical of tropical forest fires in western Amazon (Hodgson *et al* 2018, Darbyshire *et al* 2019). The underestimation of BC in the eastern region (observed: 1.4 $\mu g\,m^{-3}$; model 0.2 $\mu g\,m^{-3}$) may partly be a result of underrepresentation of emissions from Cerrado fires in eastern regions. However, we note the few flights were undertaken in the eastern region compared to western region (section 2.3.3).

3.3. AOD

Figure 5 shows daily mean simulated and observed AOD at 500 nm (AOD500) between May and December 2012 at five AERONET stations located in western and southern Amazon Basin. Measured AOD500 is typically <0.2 in May and June, increasing to 0.4 to 1.5 in August and September, reducing to <0.2 in December. The model captures this seasonal cycle relatively well (r = 0.61 to 0.88). May to December mean AOD500 is overestimated in western locations (Rio Branco, NMBF = 0.53, Porto Velho UNIR (NMBF = 0.47) and Santa Cruz UTEPSA (NMBF = 0.47), and well simulated compared to more eastern locations: Alta Floresta (NMBF = 0.03) and Cuiabá-Miranda (NMBF = −0.01).

Comparison against AOD at 550 nm retrieved by MODIS (AOD550), confirms the model overestimates in the western Amazon and underestimates eastern regions (supplementary figure 4). AERONET AOD500 and MODIS AOD550 are found to compare well (supplementary figure 5) despite the different wavelengths.

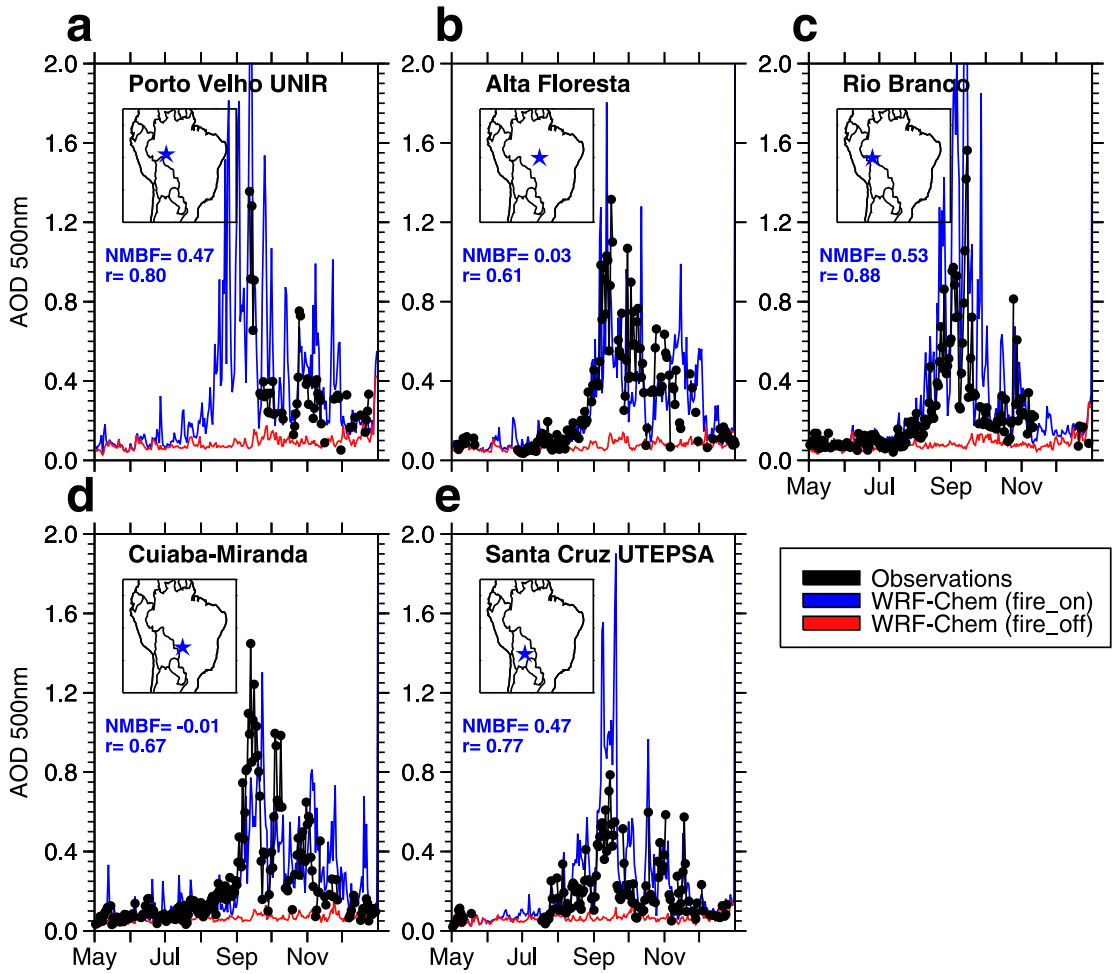

Figure 5. Daily mean observed (black circles) and simulated (coloured lines) aerosol optical depth (AOD) at 500 nm at five AERONET stations. (a) Porto Velho UNIR (8.84 °S, 63.94 °W). (b) Alta Floresta (9.87 °S, 56.10 °W). (c) Rio Branco (9.96 °S, 67.87 °W). (d) Cuiabá-Miranda (15.73 °S, 56.02 °W). (e) Santa Cruz UTEPSA (17.77 °S, 63.20 °W).

Evaluating against MODIS separately over evergreen broadleaf forest and savannah (cerrado) biomes and across the western and eastern regions shows an overall very small low bias in western forest bias regions with an equally small high bias in eastern cerrado regions (supplementary figure 6). The underestimation over savannah regions is considerably less than the underestimate against the one aircraft flight in the east, suggesting comparison against this one flight may not be representative. However, Reddington *et al* (2019b) also found PM and AOD were underestimated over regions with savannah and grassland fires, possibly suggesting FINN underestimates fire emissions in these regions.

3.4. Fire impacts on simulated $PM_{2.5}$ and burden of disease

Some previous modelling studies of Amazon (Archer-Nicholls *et al* 2015, Johnson *et al* 2016) and other tropical fires (see Reddington *et al* (2019b) for a review) underestimate AOD and scale-up fire emissions to enable the model to match observed AOD. We find a consistent evaluation of regional boundary layer PM concentrations and AOD, with a slight overestimation over forested regions in the western Amazon and underestimation over savanna regions. Overall, simulated $PM_{2.5}$ was typically within 25% of measurements both close to fires in the western Amazon and in urban regions far from fires. We therefore chose not to alter fire emissions and we use $PM_{2.5}$ concentrations from the model runs with and without fire emissions to estimate impacts on human health.

Figure 6 shows simulated surface dry season $PM_{2.5}$ concentrations. Greatest dry season concentrations ($\geqslant$45 $\mu g\,m^{-3}$) occur in the southern and western Amazon. Vegetation fires contribute up to 80%–95% of simulated dry season $PM_{2.5}$ concentrations, with contributions >60% over most of the Brazilian Amazon, Bolivia, and much of Peru and Paraguay.

Figure 7 shows the regional distribution of dry season mean simulated $PM_{2.5}$ concentrations. Vegetation fires increased regional mean $PM_{2.5}$ concentrations by 260% over the Amazon Basin in 2012, exposing

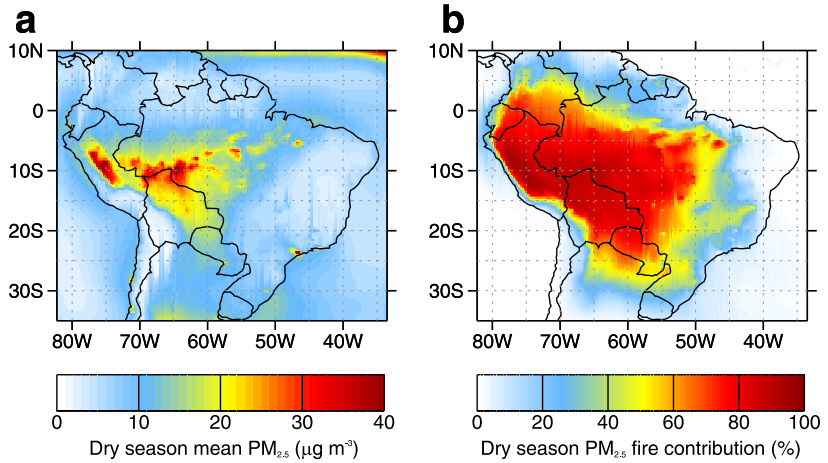

Figure 6. Simulated dry season (August to October) surface $PM_{2.5}$ concentrations in 2012. (a) $PM_{2.5}$ concentrations (b) percentage contribution due to fires.

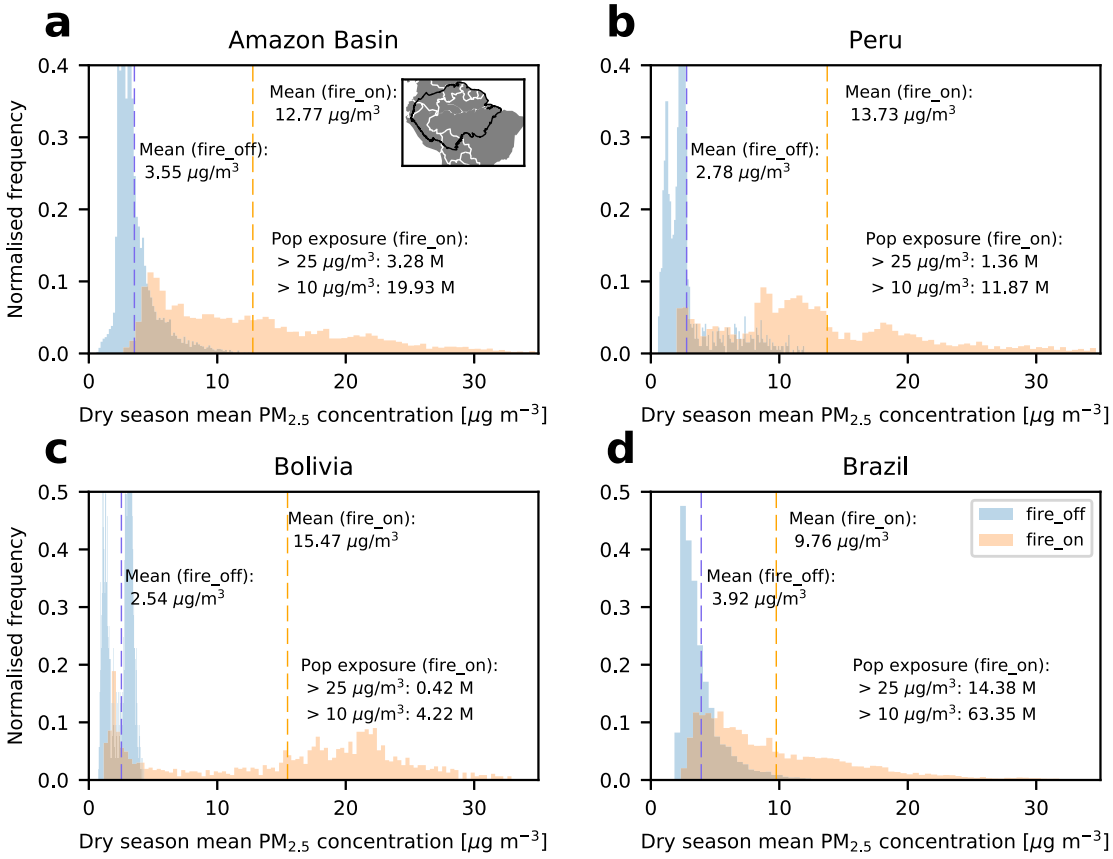

Figure 7. Simulated distribution of dry season (August to October) surface $PM_{2.5}$ concentrations in 2012. (a) Amazon Basin, (b) Peru, (c) Bolivia, and (d) Brazil. Histograms show mean $PM_{2.5}$ distribution for WRF-Chem simulations with (fire_on) and without (fire_off) fire emissions, with vertical dashed lines representing the distribution mean for each simulation. The number of people exposed (in millions M) to mean concentrations above 25 (WHO 24-h guideline) and 10 (WHO annual guideline) $\mu g\,m^{-3}$ is also shown.

20 million people to dry season mean concentrations above 10 $\mu g\,m^{-3}$ and 3.3 million people to concentrations over 25 $\mu g\,m^{-3}$. Similarly large increases are also simulated at the national scale for Peru (394%) and Bolivia (509%) where 7% (1.36 million people) and 4% (0.42 million people) are exposed to $PM_{2.5}$ levels above 25 $\mu g\,m^{-3}$, respectively. Fires have a marked impact on annual concentrations and thus chronic exposure (see also supplementary figure 7), increasing annual mean population-weighed $PM_{2.5}$ concentrations by 35% and 137% in Peru and Bolivia, respectively (table 2). By comparison, vegetation fires increased the national

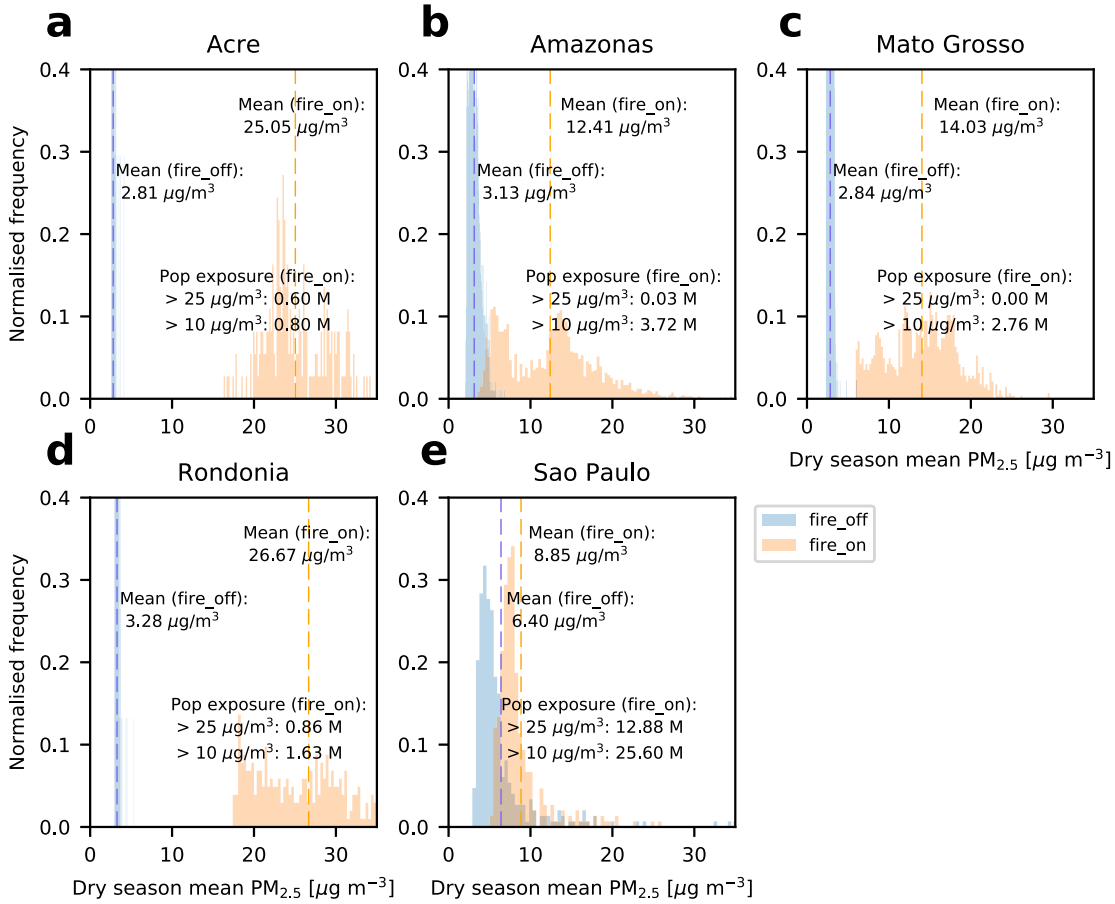

Figure 8. Simulated distribution of regional dry season (August to October) surface $PM_{2.5}$ concentrations in 2012 for five Brazilian states. (a) Acre, (b) Amazonas, (c) Mato Grosso, (d) Rondônia, and (e) São Paulo. Histograms show mean $PM_{2.5}$ distribution for WRF-Chem simulations with (fire_on) and without (fire_off) fire emissions, with vertical dashed lines representing the distribution mean for each simulation. The number of people exposed (in millions M) to mean concentrations above 25 (WHO 24-h guideline) and 10 (WHO annual guideline) $\mu g\,m^{-3}$ is also shown.

Table 2. Annual mean population-weighted $PM_{2.5}$ concentrations in 2012 for WRF-Chem simulation (fire_on). Values in parentheses show the increase to due vegetation fires.

Country	Pop-weighted $PM_{2.5}$ ($\mu g\,m^{-3}$)
Bolivia	4.1 (137%)
Brazil	10.3 (10%)
Peru	6.2 (35%)
Brazilian state	
Acre	10.5 (222%)
Amazonas	9.2 (59%)
Mato Grosso	7.5 (168%)
Rondônia	10.4 (278%)
São Paulo	19.9 (5%)

regional dry season mean $PM_{2.5}$ by a smaller amount in Brazil (148%) in 2012, exposing 14.4 million people to levels above 25 $\mu g\,m^{-3}$ in the dry season, increasing annual mean population-weighed $PM_{2.5}$ concentrations by 10%.

Due to the proximity of fires, western states of Brazil are impacted by fires disproportionately. Figure 8 shows regional distribution of dry season mean simulated $PM_{2.5}$ concentrations in four western states of Brazil (Acre, Amazonas, Mato Grosso, and Rondônia) and the state of São Paulo in south-eastern Brazil. Vegetation fires increase regional $PM_{2.5}$ concentrations considerably in western states (296%–791%), exposing the majority of state populations to dry season mean $PM_{2.5}$ concentrations above 25 $\mu g\,m^{-3}$ in Rondônia (53%) and Acre (75%). Fires similarly increase annual mean population-weighted $PM_{2.5}$ concentrations considerably in these western states (59%–278%), highlighting the impact on chronic exposures. In contrast, exposure to unhealthy

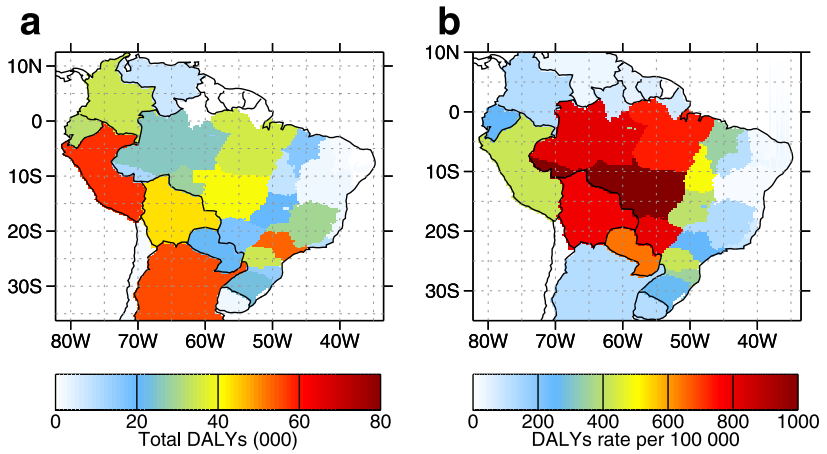

Figure 9. The averted burden of disease due to the prevention of vegetation fires in 2012 using the GEMM NCD + LRI exposure-response function. (a) Total averted disability-adjusted life years (DALYs), and (b) averted DALYs as rate per 100,000 persons.

Table 3. Averted burden of disease due to the prevention of vegetation fires in 2012 using the GEMM NCD + LRI exposure-response function. Values shown are estimates using the 'substitution' method.

Country	DALYs	DALYs rate per 100 000	Mortality	Mortality rate per 100 000
Argentina	55 065 (48 341–62 787)	121 (106–138)	1 806 (1 765–1849)	4 (4–4)
Bolivia	43 320 (33 246–53 764)	789 (605–979)	1 195 (985–1 409)	21.8 (18–26)
Brazil	385 173 (338 408 –438 639)	597 (524–680)	9 774 (9 686–9 865)	15.1 (15–15)
Chile	1 053 (910–1 219)	3 (3–4)	29 (29–29)	0.1 (0–0.1)
Colombia	34 096 (29 290–39 703)	124 (107–145)	866 (854–879)	3.2 (3–3.3)
Ecuador	32 394 (27 610–37 806)	256 (218–299)	861 (822–900)	7 (7–7)
Guyana	138 (121–159)	43 (37–49)	4 (4–4)	1 (1–1)
Paraguay	21 978 (18 139–26 371)	644 (531–772)	555 (503–613)	16.2 (15–18)
Peru	57 947 (47 378–69 587)	422 (345–506)	1 467 (1 336–1 591)	11 (10–12)
Suriname	289 (247–337)	58 (50–68)	8 (7–9)	1.6 (2–2)
Uruguay	2 293 (2 031–2 595)	120 (106–136)	83 (82–85)	4 (4–4)
Venezuela	7 186 (6 174–8 336)	34 (30–40)	195 (185–204)	1 (1–1)
Total	640 938 (551 892–741 303)	—	16 845 (16 256–17 437)	—
Amazon Basin:	168 000 (143 800–194 900)		4 300 (4 100–4 500)	

$PM_{2.5}$ concentrations in outflow regions such as São Paulo is largely due to other anthropogenic emissions with fires playing a limited intermittent contribution. Nevertheless fires can contribute to very high concentrations in outflow regions, leading to a 39% increase in dry season regional mean concentrations and a 5% increase in annual mean population-weighted concentrations in São Paulo.

Figure 9 shows the estimated reduction in the regional burden of disease that would occur if all vegetation fires were prevented. We estimate that the prevention of vegetation fire emissions had the potential to avoid 641 00 (95UI: 551 900–741 300) DALYs and 16 800 (95UI: 16 300–17 400) premature deaths across our South American domain in 2012. We found that approximately 26% of the avoided DALYs (167 900 (95UI: 143 800–194 900)) and deaths (4 300 (95UI: 4 100–4 500)) due to fire prevention were located inside the Amazon Basin. At the national level, preventing vegetation fires could have prevented 9 770 (95UI: 9 690–9 870) premature mortalities in Brazil, 1 467 (95UI: 1 340–1 590) in Peru and 1 195 (95UI: 985–1 410) in Bolivia (table 3). Per capita health burdens remove population size dependence highlighting the impact of fires on public health. The per capita avoided heath burden is greatest in Bolivia (789 (95UI: 605–979) DALYs per 100 000 people) and Paraguay (644 (95UI: 531–772) DALYs per 100 000 people) followed by Brazil (597 (95UI: 524–680) DALYs per 100 000 people). Brazilian states of Rondônia, Acre, and Mato Grosso benefit the most from fire prevention with 1300–1800 DALYs per 100 000 people avoided (figure 9 and supplementary table 4). High disease burden rates in these western Brazilian states and wider Amazon Basin, highlights the adverse impact of vegetation fires on regional public health.

Our estimated health impacts are consistent with previous estimates for South America from global models but provide advancement due to the use of a high resolution regional model and updated exposure-response relationships. Johnston *et al* (2012) estimated preventing fires would avoid 10 000 premature deaths annually

between 1997–2006. Reddington *et al* (2015) estimated prevention of vegetation fires would avert ~7000 to 9700 premature deaths annually between 2002–2011.

In contrast to the Amazon Basin and the wider South American region, numerous air quality health assessments due to vegetation fires have been conducted across Equatorial Asia. Marlier *et al* (2019) found the prevention of fires across Equatorial Asia (Indonesia, Malaysia, and Singapore) would avert 24 000 premature deaths annually in the present-day. Using a similar WRF-Chem setup as used in this study, Reddington *et al* (2019a) estimated the prevention of fires would avoid 8,000 premature deaths annually across Southeast Asia (Myanmar, Thailand, Laos, Cambodia, and Vietnam) in the present-day. Using a similar WRF-Chem setup as used in this study, Kiely *et al* (2020) found that the prevention of vegetation and peat fires would avert 15 000 premature deaths and 500 000 DALYs annually in 2004, 2006, and 2009 across Equatorial Asia. A number of studies focused on 2015, where drought induced fires resulted in a major haze event across Equatorial Asia, and caused an estimated 44 000–100 300 premature mortalities (Crippa *et al* 2016, Koplitz *et al* 2016, Kiely *et al* 2020).

Calculated health burdens are sensitive to both simulated PM exposure and exposure-response relationships (Ostro *et al* 2018, Burnett and Cohen 2020). For the 2015 haze event in Equatorial Asia, Kiely *et al* (2020) found that exposure-outcome associations have the largest influence on health impact estimates. Kiely *et al* (2020) used the same exposure-outcome association as this study (GEMM NCD + LRI) and estimated 44,000 premature deaths in 2015. In contrast, Koplitz *et al* (2016) used an exposure-outcome association based on work from Schwartz *et al* (2008), Anenberg *et al* (2012), Lepeule *et al* (2012), with a 1% in all-cause mortality per 1 $\mu g\,m^{-3}$ increase in annual average PM2.5 concentrations. Koplitz *et al* (2016) estimated 100,300 premature deaths in 2015. When Kiely *et al* (2020) used the same exposure-outcome association they estimated a similar premature death estimate of 106,000 deaths in 2015. Marlier *et al* (2019) also used a similar exposure-outcome association to that used in Koplitz *et al* (2016), based on work from Vodonos *et al* (2018).

Both the Vodonos *et al* (2018) exposure-outcome association and the GEMM NCD + LRI rely on epidemiological studies from ambient $PM_{2.5}$ exposure only, including some from high-exposure locations, and include all non-accidental causes of death. The current integrated exposure-response (IER) association from Global Burden of Disease GBD2017 is based on studies of ambient and household air pollution, passive smoking, and active smoking exposures and is cause-specific for six causes of death (Burnett *et al* 2014). The risk responses of Vodonos *et al* (2018) and the GEMM NCD + LRI are similar for exposures up to 50 $\mu g\,m^{-3}$. At exposures greater than 50 $\mu g\,m^{-3}$ these functions diverge, with the GEMM NCD + LRI risk flattening off at higher concentrations. The IER has lower risks than either Vodonos *et al* (2018) and the GEMM NCD + LRI, and flattens off at lower concentrations. For example, Nawaz and Henze (2020) estimated 4 407 premature deaths per year on average between 2016 and 2019 in Brazil from biomass burning derived ambient $PM_{2.5}$, which is approximately half of our estimate for Brazil in 2012, primarily due to their use of the IER from GBD2016 which has approximately half the attributable risks of the GEMM NCD + LRI that we used in this study.

These large differences emphasise the need to reduce these uncertainties and for further epidemiological studies from highly polluted regions of the world (Burnett and Cohen 2020, Pope *et al* 2020). We used the GEMM NCD + LRI here to be consistent with the latest exposure-outcome associations for ambient $PM_{2.5}$ exposure only, to include causes beyond that considered by the current IER in the GBD2017, and to be conservative of risk estimates at higher exposures.

Fire emissions in the tropics depend on land-use change and climate conditions and can exhibit strong interannual variability. Reddington *et al* (2015) found greater health impacts in years with greater fires due to drought or deforestation. Fire emissions in the Amazon in 2012 were comparable to the 11-y average (figure 1). Years with more fires, due either to drought conditions or greater deforestation and land-use change, would have greater emissions, PM concentrations and likely greater associated public health impacts. Future work is needed to understand the year to year variability in health impacts due to PM from fires in the region.

4. Conclusion

We used a high-resolution regional air quality model to assess the impacts of vegetation fires on regional South American air quality and estimate the public health benefits resulting from prevention of fires. We studied 2012, a year with emissions similar to the long-term (2008 to 2018) average. $PM_{2.5}$ and AOD was evaluated against a comprehensive set of surface, aircraft and satellite measurements, with model typically matching measurements within 25%. Fires are the dominant pollution source, contributing more than 80% of surface $PM_{2.5}$ concentrations across the southern Amazon during the dry season. Fires in the Amazon account for ~70% of fire emissions across our South American domain and 12% of global fire emissions.

We found that the prevention of vegetation fires in the region would avert 641 000 (95UI: 551 900–741 300) DALYs and 16 800 (95UI: 16 300–17 400) premature deaths due to the reduction in $PM_{2.5}$ exposure across South America. The greatest reduction in disease burden rates occurs in regions close to intense fire activity: Bolivia, Paraguay, and the western states of Brazil, including Rondônia, Acre, and Mato Grosso, with 26% of the avoided health burden located within the Amazon Basin. We find that exposure to PM from fires in the Amazon has a similar public health impacts to fires in Equatorial Asia, which have been more extensively studied. Our analysis highlights the substantial public health benefits that could be achieved through prevention of vegetation fires across the Amazon. Future work needs to quantify the air quality degradation specifically caused by fires associated with deforestation and forest degradation, providing further evidence for the health benefits that would result from reduced deforestation (Reddington *et al* 2015). The deforestation rate in the Amazon increased from 2014 to 2019 with more fires in 2019 compared to recent years (Barlow *et al* 2020). The future frequency of fire in the Amazon will depend on land-use and climate change, with projected increases in fire occurrence of 20%–100% over the coming decades (Fonseca *et al* 2019). Achieving reductions in fire in a hotter and potentially drier Amazon (Boisier *et al* 2015) will require strong environmental governance.

Acknowledgments

This work received funding from the Natural Environment Research Council (NERC) through the SAMMBA project (NE/J009822/1; NE/J010073/1) and the European Research Council (ERC) under the European Union's Horizon 2020 research and innovation programme (Grant agreement No. 771492). We acknowledge support from the United Bank of Carbon (UBoC) and Spracklen acknowledges support from a Philip Leverhulme Prize. Reddington was supported by AIA Group. This work was undertaken on Advanced Research Computing, part of the High Performance Computing facilities at the University of Leeds, UK.

ORCID iDs

Edward W Butt https://orcid.org/0000-0002-6087-4848
Dominick V Spracklen https://orcid.org/0000-0002-7551-4597

References

Akagi S, Yokelson R J, Wiedinmyer C, Alvarado M, Reid J, Karl T, Crounse J and Wennberg P 2011 Emission factors for open and domestic biomass burning for use in atmospheric models *Atmos. Chem. Phys.* **11** 4039–72

Akagi S, Yokelson R J, Burling I, Meinardi S, Simpson I, Blake D R, Mcmeeking G, Sullivan A, Lee T and Kreidenweis S 2013 Measurements of reactive trace gases and variable O_3 formation rates in some South Carolina biomass burning plumes *Atmos. Chem. Phys.* **13** 1141–65

Alencar A A, Brando P M, Asner G P and Putz F E 2015 Landscape fragmentation, severe drought, and the new Amazon forest fire regime *Ecological Applications* **25** 1493–505

Allan J D, Morgan W T, Darbyshire E, Flynn M J, Williams P I, Oram D E, Artaxo P, Brito J, Lee J D and Coe H 2014 Airborne observations of IEPOX-derived isoprene SOA in the Amazon during SAMBBA *Atmos. Chem. Phys.* **14** 11393–407

Anenberg S C, Schwartz J, Shindell D, Amann M, Faluvegi G, Klimont Z, Janssens-Maenhout G, Pozzoli L, van Dingenen R and Vignati E 2012 Global air quality and health co-benefits of mitigating near-term climate change through methane and black carbon emission controls *Environ. Health Perspect.* **120** 831–9

Apte J S, Brauer M, Cohen A J, Ezzati M and Pope C A III 2018 Ambient PM2. 5 reduces global and regional life expectancy *Environmental Science & Technology Letters* **5** 546–51

Arãgao L E O, Malhi Y, Barbier N, Lima A, Shimabukuro Y, Anderson L and Saatchi S 2008 Interactions between rainfall, deforestation and fires during recent years in the Brazilian Amazonia *Philosophical Transactions of the Royal Society B: Biological Sciences* **363** 1779–85

Aragão L E, Anderson L O, Fonseca M G, Rosan T M, Vedovato L B, Wagner F H, Silva C V, Junior C H S, Arai E and Aguiar A P 2018 21st century drought-related fires counteract the decline of Amazon deforestation carbon emissions *Nat. Commun.* **9** 1–12

Archer-Nicholls S, Lowe D, Darbyshire E, Morgan W, Bela M, Pereira G, Trembath J, Kaiser J, Longo K and Freitas S 2015 Characterising Brazilian biomass burning emissions using WRF-Chem with MOSAIC sectional aerosol *Geoscientific Model Development* **8** 549–77

Archer-Nicholls S, Lowe D, Schultz D M and Mcfiggans G 2016 Aerosol–radiation–cloud interactions in a regional coupled model: the effects of convective parameterisation and resolution *Atmos. Chem. Phys.* **16** 5573

Artaxo P, Rizzo L V, Brito J F, Barbosa H M, Arana A, Sena E T, Cirino G G, Bastos W, Martin S T and Andreae M O 2013 Atmospheric aerosols in Amazonia and land use change: from natural biogenic to biomass burning conditions *Faraday Discuss.* **165** 203–35

Baker J and Spracklen D 2019 Climate benefits of intact Amazon forests and the biophysical consequences of disturbance *Frontiers in Forests and Global Change* **2** 47

Barlow J, Berenguer E, Carmenta R and França F 2020 Clarifying Amazonia's burning crisis *Global Change Biology* **26** 319–21

Boisier J P, Ciais P, Ducharne A and Guimberteau M 2015 Projected strengthening of Amazonian dry season by constrained climate model simulations *Nat. Clim. Change* **5** 656–60

Brito J, Rizzo L V, Morgan W T, Coe H, Johnson B, Haywood J, Longo K, Freitas S, Andreae M O and Artaxo P 2014 Ground-based aerosol characterization during the South American Biomass Burning Analysis (SAMBBA) field experiment *Atmos. Chem. Phys.* **14** 12069–83

Burnett R T, Pope C A III, Ezzati M, Olives C, Lim S S, Mehta S, Shin H H, Singh G, Hubbell B and Brauer M 2014 An integrated risk function for estimating the global burden of disease attributable to ambient fine particulate matter exposure *Environ. Health Perspect.* **122** 397–403

Burnett R, Chen H, Szyszkowicz M, Fann N, Hubbell B, Pope C A, Apte J S, Brauer M, Cohen A and Weichenthal S 2018 Global estimates of mortality associated with long-term exposure to outdoor fine particulate matter *Proc. Natl Acad. Sci.* **115** 9592–7

Burnett R and Cohen A 2020 Relative risk functions for estimating excess mortality attributable to outdoor PM2. 5 air pollution: evolution and state-of-the-art *Atmosphere* **11** 589

Canagaratna M, Jayne J, Jimenez J, Allan J, Alfarra M, Zhang Q, Onasch T, Drewnick F, Coe H and Middlebrook A 2007 Chemical and microphysical characterization of ambient aerosols with the aerodyne aerosol mass spectrometer *Mass Spectrom. Rev.* **26** 185–222

Cano-Crespo A, Oliveira P J, Boit A, Cardoso M and Thonicke K 2015 Forest edge burning in the Brazilian Amazon promoted by escaping fires from managed pastures *Journal of Geophysical Research: Biogeosciences* **120** 2095–107

Chin M, Rood R B, Lin S J, Müller J F and Thompson A M 2000 Atmospheric sulfur cycle simulated in the global model GOCART: model description and global properties *Journal of Geophysical Research: Atmospheres* **105** 24671–87

Cohen A J, Brauer M, Burnett R, Anderson H R, Frostad J, Estep K, Balakrishnan K, Brunekreef B, Dandona L and Dandona R 2017 Estimates and 25-year trends of the global burden of disease attributable to ambient air pollution: an analysis of data from the Global Burden of Diseases Study 2015 *The Lancet* **389** 1907–18

Conibear L, Butt E W, Knote C, Arnold S R and Spracklen D V 2018 Residential energy use emissions dominate health impacts from exposure to ambient particulate matter in India *Nat. Commun.* **9** 1–9

Crippa P, Castruccio S, Archer-Nicholls S, Lebron G, Kuwata M, Thota A, Sumin S, Butt E, Wiedinmyer C and Spracklen D 2016 Population exposure to hazardous air quality due to the 2015 fires in Equatorial Asia *Sci. Rep.* **6** 37074

da Silva S S, Fearnside P M, de Alencastro Graça P M L, Brown I F, Alencar A and de Melo A W F 2018 Dynamics of forest fires in the southwestern Amazon *Forest Ecology and Management* **424** 312–22

Darbyshire E, Morgan W T, Allan J D, Liu D, Flynn M J, Dorsey J R, O'shea S J, Lowe D, Szpek K and Marenco F 2019 The vertical distribution of biomass burning pollution over tropical South America from aircraft *in situ* measurements during SAMBBA *Atmos. Chem. Phys.* **19** 5771–90

de Oliveira Alves N, Vessoni A T, Quinet A, Fortunato R S, Kajitani G S, Peixoto M S, de Souza Hacon S, Artaxo P, Saldiva P and Menck C F M 2017 Biomass burning in the Amazon region causes DNA damage and cell death in human lung cells *Sci. Rep.* **7** 10937

Dee D P, Uppala S, Simmons A, Berrisford P, Poli P, Kobayashi S, Andrae U, Balmaseda M, Balsamo G and Bauer D P 2011 The ERA-Interim reanalysis: configuration and performance of the data assimilation system *Q. J. R. Meteorolog. Soc.* **137** 553–97

Dentener F, Kinne S, Bond T, Boucher O, Cofala J, Generoso S, Ginoux P, Gong S, Hoelzemann J and Ito A 2006 Emissions of primary aerosol and precursor gases in the years 2000 and 1750 prescribed data-sets for AeroCom *Atmos. Chem. Phys.* **6** 4321–44

Do Carmo C N, Alves M B and de Souza Hacon S 2013 Impact of biomass burning and weather conditions on children's health in a city of Western Amazon region *Air Quality, Atmosphere & Health* **6** 517–25

Doxsey-Whitfield E, Macmanus K, Adamo S B, Pistolesi L, Squires J, Borkovska O and Baptista S R 2015 Taking advantage of the improved availability of census data: a first look at the gridded population of the world, version 4 *Papers in Applied Geography* **1** 226–34

Emmons L K *et al* 2010 Description and Evaluation of the Model for Ozone and Related chemical Tracers *Geosci. Model Dev.* **3** 43–67 version 4 (MOZART-4)

Fonseca M G, Alves L M, Aguiar A P D, Arai E, Anderson L O, Rosan T M, Shimabukuro Y E and de Aragão L E O E C 2019 Effects of climate and land-use change scenarios on fire probability during the 21st century in the Brazilian Amazon *Global Change Biol.* **25** 2931–46

Freitas S R, Longo K M, Chatfield R, Latham D, Silva Dias M, Andreae M, PRINS E, Santos J, Gielow R and Carvalho J Jr 2007 Including the sub-grid scale plume rise of vegetation fires in low resolution atmospheric transport models *Atmos. Chem. Phys.* **7** 3385–98

Fromm M, Alfred J, Hoppel K, Hornstein J, Bevilacqua R, Shettle E, Servranckx R, Li Z and Stocks B 2000 Observations of boreal forest fire smoke in the stratosphere by POAM III, SAGE II, and lidar in 1998 *Geophys. Res. Lett.* **27** 1407–10

Giglio L, Descloitres J, Justice C O and Kaufman Y J 2003 An enhanced contextual fire detection algorithm for MODIS *Remote Sens. Environ.* **87** 273–82

Giglio L 2007 Characterization of the tropical diurnal fire cycle using VIRS and MODIS observations *Remote Sens. Environ.* **108** 407–21

Giles D M, Sinyuk A, Sorokin M G, Schafer J S, Smirnov A, Slutsker I, Eck T F, Holben B N, Lewis J R and Campbell J R 2019 Advancements in the Aerosol Robotic Network (AERONET) Version 3 database–automated near-real-time quality control algorithm with improved cloud screening for Sun photometer aerosol optical depth (AOD) measurements *Atmos. Meas. Tech.* **12** 169–209

Gonzalez-Alonso L, VAL Martin M and Kahn R A 2019 Biomass-burning smoke heights over the Amazon observed from space *Atmos. Chem. Phys.* **19** 1685–702

Grell G A and Dévényi D 2002 A generalized approach to parameterizing convection combining ensemble and data assimilation techniques *Geophys. Res. Lett.* **29** 38-1-38-4

Grell G A, Peckham S E, Schmitz R, Mckeen S A, Frost G, Skamarock W C and Eder B 2005 Fully coupled 'online' chemistry within the WRF model *Atmos. Environ.* **39** 6957–75

Guenther A, Karl T, Harley P, Wiedinmyer C, Palmer P and Geron C 2006 Estimates of global terrestrial isoprene emissions using MEGAN (Model of Emissions of Gases and Aerosols from Nature) *Atmos. Chem. Phys.* **6** 3181–210

Heald C L and Spracklen D V 2015 Land use change impacts on air quality and climate *Chem. Rev.* **115** 4476–96

Hijmans R, Garcia N, Kapoor J, Rala A, Maunahan A and Wieczorek J 2012 *Global Administrative Areas (Boundaries)* (Berkeley: Museum of Vertebrate Zoology and the International Rice Research Institute, University of California)

Hodgson A K, Morgan W T, O'shea S, Bauguitte S, Allan J D, Darbyshire E, Flynn M J, Liu D, Lee J and Johnson B 2018 Near-field emission profiling of tropical forest and Cerrado fires in Brazil during SAMBBA 2012 *Atmos. Chem. Phys.* **18** 5619–38

Hodzic A and Knote C 2014 WRF-Chem 3.6. 1: MOZART gas-phase chemistry with MOSAIC aerosols *Atmospheric Chemistry Division (ACD), National Center for Atmospheric Research (NCAR)* **7**

Holben B N, Eck T F, Slutsker I, Tanre D, Buis J, Setzer A, Vermote E, Reagan J A, Kaufman Y and Nakajima T 1998 AERONET—a federated instrument network and data archive for aerosol characterization *Remote Sens. Environ.* **66** 1–16

Huang K, Fu J S, Hsu N C, Gao Y, Dong X, Tsay S-C and Lam Y F 2013 Impact assessment of biomass burning on air quality in Southeast and East Asia during BASE-ASIA *Atmos. Environ.* **78** 291–302

Ignotti E, Valente J G, Longo K M, Freitas S R, Hacon S D S and Artaxo Netto P 2010 Impact on human health of particulate matter emitted from burnings in the Brazilian Amazon region *Revista de Saude Publica* **44** 121–30

Jacobson L D S V, de Souza Hacon S, de Castro H A, Ignotti E, Artaxo P and de Leon A C M P 2012 Association between fine particulate matter and the peak expiratory flow of schoolchildren in the Brazilian subequatorial Amazon: a panel study *Environ. Res.* **117** 27–35

Jacobson L D S V, de Souza Hacon S, de Castro H A, Ignotti E, Artaxo P, Saldiva P H N and de Leon A C M P 2014 Acute effects of particulate matter and black carbon from seasonal fires on peak expiratory flow of schoolchildren in the Brazilian Amazon *PLoS One* **9** e104177
Janssens-Maenhout G, Crippa M, Guizzardi D, Dentener F, Muntean M, Pouliot G, Keating T, Zhang Q, Kurokawa J and Wankmüller R 2015 HTAP_v2. 2: a mosaic of regional and global emission grid maps for 2008 and 2010 to study hemispheric transport of air pollution *Atmos. Chem. Phys.* **15** 11411–32
Johnston F H, Henderson S B, Chen Y, Randerson J T, Marlier M, Defries R S, Kinney P, Bowman D M and Brauer M 2012 Estimated global mortality attributable to smoke from landscape fires *Environ. Health Perspect.* **120** 695–701
Johnson B T *et al* 2016 Evaluation of biomass burning aerosols in the HadGEM3 climate model with observations from the SAMBBA field campaign *Atmos. Chem. Phys.* **16** 14657–85
Kaiser J W *et al* 2012 Biomass burning emissions estimated with a global fire assimilation system based on observed fire radiative power *Biogeosciences* **9** 527
Kiely L, Spracklen D V, Wiedinmyer C, Conibear L, Reddington C L, Archer-Nicholls S, Lowe D, Arnold S R, Knote C and Khan M F 2019 New estimate of particulate emissions from Indonesian peat fires in 2015 *Atmos. Chem. Phys.* **19** 11105–21
Kiely L *et al* 2020 Air quality and health impacts of vegetation and peat fires in Equatorial Asia during 2004—2015 *Environmental Research Letters* **15** 094054
Kim P S, Jacob D J, Mickley L J, Koplitz S N, Marlier M E, Defries R S, Myers S S, Chew B N and Mao Y H 2015 Sensitivity of population smoke exposure to fire locations in Equatorial Asia *Atmos. Environ.* **102** 11–7
Knote C, Hodzic A, Jimenez J, Volkamer R, Orlando J, Baidar S, Brioude J, Fast J, Gentner D and Goldstein A 2014 Simulation of semi-explicit mechanisms of SOA formation from glyoxal in aerosol in a 3D model *Atmos. Chem. Phys.* **14** 6213–39
Knote C, Hodzic A and Jimenez J 2015 The effect of dry and wet deposition of condensable vapors on secondary organic aerosols concentrations over the continental US *Atmos. Chem. Phys.* **15** 1–18
Kodros J K, Wiedinmyer C, Ford B, Cucinotta R, Gan R, Magzamen S and Pierce J R 2016 Global burden of mortalities due to chronic exposure to ambient PM2. 5 from open combustion of domestic waste *Environ. Res. Lett.* **11** 124022
Kolusu S, Marsham J, Mulcahy J, Johnson B, Dunning C, Bush M and Spracklen D 2015 Impacts of Amazonia biomass burning aerosols assessed from short-range weather forecasts *Atmos. Chem. Phys.* **15** 12251–66
Koplitz S N, Mickley L J, Marlier M E, Buonocore J J, Kim P S, Liu T, Sulprizio M P, Defries R S, Jacob D J and Schwartz J 2016 Public health impacts of the severe haze in Equatorial Asia in September–October 2015: demonstration of a new framework for informing fire management strategies to reduce downwind smoke exposure *Environ. Res. Lett.* **11** 094023
Lelieveld J, Evans J S, Fnais M, Giannadaki D and Pozzer A 2015 The contribution of outdoor air pollution sources to premature mortality on a global scale *Nature* **525** 367
Lepeule J, Laden F, Dockery D and Schwartz J 2012 Chronic exposure to fine particles and mortality: an extended follow-up of the Harvard Six Cities study from 1974 to 2009 *Environ. Health Perspect.* **120** 965–70
Levy R, Mattoo S, Munchak L, Remer L, Sayer A, Patadia F and Hsu N 2013 The Collection 6 MODIS aerosol products over land and ocean *Atmos. Meas. Tech.* **6** 2989
Lipsett M J, Ostro B D, Reynolds P, Goldberg D, Hertz A, Jerrett M, Smith D F, Garcia C, Chang E T and Bernstein L 2011 Long-term exposure to air pollution and cardiorespiratory disease in the California teachers study cohort *American Journal of Respiratory and Critical Care medicine* **184** 828–35
Liu L *et al* 2020 Impact of biomass burning aerosols on radiation, clouds, and precipitation over the Amazon during the dry season: dependence of aerosol-cloud and aerosol-radiation interactions on aerosol loading *Atmos. Chem. Phys. Discuss.* (https://doi.org/10.5194/acp-2020-191)
Lovejoy T E and Nobre C 2018 Amazon tipping point *Sci. Adv.* **4** eaat2340
Machado-Silva F, Libonati R, de Lima T F M, Peixoto R B, de Almeida França J R, Magalhães M D A F M, Santos F L M, Rodrigues J A and Dacamara C C 2020 Drought and fires influence the respiratory diseases hospitalizations in the Amazon *Ecol. Indic.* **109** 105817
Marenco F *et al* 2016 On the vertical distribution of smoke in the amazonian atmosphere during the dry season *Atmos. Chem. Phys.* **16** 2155–74
Marlier M E, Defries R S, Kim P S, Koplitz S N, Jacob D J, Mickley L J and Myers S S 2015 Fire emissions and regional air quality impacts from fires in oil palm, timber, and logging concessions in Indonesia *Environ. Res. Lett.* **10** 085005
Marlier M E *et al* 2019 Fires, smoke exposure, and public health: an integrative framework to maximize health benefits from peatland restoration *GeoHealth* **3** 178–89
Martin S T *et al* 2010 Sources and properties of Amazonian aerosol particles *Reviews of Geophysics* **48**
Miller K A, Siscovick D S, Sheppard L, Shepherd K, Sullivan J H, Anderson G L and Kaufman J D 2007 Long-term exposure to air pollution and incidence of cardiovascular events in women *New Engl. J. Med.* **356** 447–58
Mishra A K, Lehahn Y, Rudich Y and Koren I 2015 Co-variability of smoke and fire in the Amazon basin *Atmos. Environ.* **109** 97–104
Morgan W T *et al* 2019a Transformation and aging of biomass burning carbonaceous aerosol over tropical South America from aircraft *in situ* measurements during SAMBBA *Atmos. Chem. Phys.* **20** 5309–26
Morgan W T, Darbyshire E, Spracklen D V, Artaxo P and Coe H 2019b Non-deforestation drivers of fires are increasingly important sources of aerosol and carbon dioxide emissions across Amazonia *Sci. Rep.* **9** 1–15
Morrison H, Thompson G and Tatarskii V 2009 Impact of cloud microphysics on the development of trailing stratiform precipitation in a simulated squall line: comparison of one-and two-moment schemes *Mon. Weather Rev.* **137** 991–1007
Nawaz M O and Henze D 2020 Premature deaths in Brazil associated with long-term exposure to PM2. 5 from Amazon fires between 2016–2019 *GeoHealth* **4** e2020GH000268
NCAR 2019 *ACOM MOZART-4/GEOS-5 global model output* (http://acom.ucar.edu/wrf-chem/mozart.shtml) (UCAR 2016)
Nepstad D C, Stickler C M, Filho B S- and Merry F 2008 Interactions among Amazon land use, forests and climate: prospects for a near-term forest tipping point *Philosophical Transactions of the Royal Society B: Biological Sciences* **363** 1737–46
Olivier J, Peters J, Granier C, Petron G, Müller J F and Wallens S 2003 Present and future surface emissions of atmospheric compounds *POET report #2, EU project EVK2-1999-00011* **11** (http://accent.aero.jussieu.fr/POET_metadata.php)
Ostro B, Spadaro J V, Gumy S, Mudu P, Awe Y, Forastiere F and Peters A 2018 Assessing the recent estimates of the global burden of disease for ambient air pollution: methodological changes and implications for low-and middle-income countries *Environ. Res.* **166** 713–25
Pereira G, Siqueira R, Rosário N E, Longo K L, Freitas S R, Cardozo F S, Kaiser J W and Wooster M J 2016 Assessment of fire emission inventories during the South American Biomass Burning Analysis (SAMBBA) experiment *Atmos. Chem. Phys.* **16** 6961
Pope C A III, Coleman N, Pond Z A and Burnett R T 2020 Fine particulate air pollution and human mortality: 25+ years of cohort studies *Environ. Res.* **183** 108924

Puett R C, Hart J E, Yanosky J D, Paciorek C, Schwartz J, Suh H, Speizer F E and Laden F 2009 Chronic fine and coarse particulate exposure, mortality, and coronary heart disease in the Nurses' health study *Environ. Health Perspect.* **117** 1697–701

Reddington C, Yoshioka M, Balasubramanian R, Ridley D, Toh Y, Arnold S and Spracklen D 2014 Contribution of vegetation and peat fires to particulate air pollution in Southeast Asia *Environ. Res. Lett.* **9** 094006

Reddington C, Butt E, Ridley D, Artaxo P, Morgan W, Coe H and Spracklen D 2015 Air quality and human health improvements from reductions in deforestation-related fire in Brazil *Nat. Geosci.* **8** 768

Reddington C L, Spracklen D V, Artaxo P, Ridley D A, Rizzo L V and Arana A 2016 Analysis of particulate emissions from tropical biomass burning using a global aerosol model and long-term surface observations *Atmos. Chem. Phys.* **16** 11083–106

Reddington C L, Conibear L, Knote C, Silver B J, Li Y J, Chan C K, Arnold S R and Spracklen D V 2019a Exploring the impacts of anthropogenic emission sectors on PM2.5 and human health in South and East Asia *Atmos. Chem. Phys.* **19** 11887–910

Reddington C L, Morgan W T, Darbyshire E, Brito J, Coe H, Artaxo P, Scott C E, Marsham J and Spracklen D V 2019b Biomass burning aerosol over the Amazon: analysis of aircraft, surface and satellite observations using a global aerosol model *Atmos. Chem. Phys.* **19** 9125–52

Schwartz J, Coull B, Laden F and Ryan L 2008 The effect of dose and timing of dose on the association between airborne particles and survival *Environ. Health Perspect.* **116** 64–9

Smith L T, Aragao L E, Sabel C E and Nakaya T 2014 Drought impacts on children's respiratory health in the Brazilian Amazon *Sci. Rep.* **4** 3726

Spracklen D V, Arnold S R and Taylor C 2012 Observations of increased tropical rainfall preceded by air passage over forests *Nature* **489** 282–5

Spracklen D and Garcia-Carreras L 2015 The impact of Amazonian deforestation on Amazon basin rainfall *Geophys. Res. Lett.* **42** 9546–52

Stephens M, Turner N and Sandberg J 2003 Particle identification by laser-induced incandescence in a solid-state laser cavity *Appl. Opt.* **42** 3726–36

Thornhill G D, Ryder C L, Highwood E J, Shaffrey L C and Johnson B T 2018 The effect of South American biomass burning aerosol emissions on the regional climate *Atmos. Chem. Phys.* **18** 5321–42

Van Der Werf G R *et al* 2017 Global fire emissions estimates during 1997–2016 *Earth System Science Data* **9** 697–720

Vodonos A, Awad Y A and Schwartz J 2018 The concentration-response between long-term PM2.5 exposure and mortality; a meta-regression approach *Environ. Res.* **166** 677–89

WHO 2018 *WHO's Ambient (Outdoor) Air Quality Database—Update 2018* (World Health Organisation)

Wiedinmyer C, Akagi S, Yokelson R J, Emmons L, Al-Saadi J, Orlando J and SOJA A 2011 The Fire INventory from NCAR (FINN): a high resolution global model to estimate the emissions from open burning *Geoscientific Model Development* **4** 625

Wu L, Su H and Jiang J H 2011 Regional simulations of deep convection and biomass burning over South America: II. Biomass burning aerosol effects on clouds and precipitation *Journal of Geophysical Research: Atmospheres* **116**

Yokelson R J, Burling I, Gilman J, Warneke C, Stockwell C, Gouw J D, Akagi S, Urbanski S, Veres P and Roberts J 2013 Coupling field and laboratory measurements to estimate the emission factors of identified and unidentified trace gases for prescribed fires *Atmos. Chem. Phys.* **13** 89–116

Yu S, Eder B, Dennis R, Chu S H and Schwartz S E 2006 New unbiased symmetric metrics for evaluation of air quality models *Atmos. Sci. Lett.* **7** 26–34

Zaveri R A, Easter R C, Fast J D and Peters L K 2008 Model for simulating aerosol interactions and chemistry (MOSAIC) *Journal of Geophysical Research: Atmospheres* **113**

Zemp D C, Schleussner C-F, Barbosa H M, Hirota M, Montade V, Sampaio G, Staal A, Wang-Erlandsson L and Rammig A 2017 Self-amplified Amazon forest loss due to vegetation-atmosphere feedbacks *Nat. Commun.* **8** 1–10

Zhang Y, Fu R, Yu H, Dickinson R E, Juarez R N, Chin M and Wang H 2008 A regional climate model study of how biomass burning aerosol impacts land-atmosphere interactions over the Amazon *Journal of Geophysical Research: Atmospheres* **113**

Zhang Y, Fu R, Yu H, Qian Y, Dickinson R, Silva Dias M A F, da Silva Dias P L and Fernandes K 2009 Impact of biomass burning aerosol on the monsoon circulation transition over Amazonia *Geophysical Research Letters* **36**